Journal of
Ceramic Science
and Technology

*J. Ceram. Sci. Tech.*, **05** [01] 31-38 (2014)
DOI: 10.4416/JCST2013-00028
available online at: http://www.ceramic-science.com


# Determination of Elastic Properties for a Wound Oxide Ceramic Composite

**Y. Shi*[1], S. Hofmann[1], R. Jemmali[1], S. Hackemann [2], D. Koch[1]**

[1]Institute of Structures and Design, German Aerospace Center Stuttgart,
Pfaffenwaldring 38 – 40, D-70569 Stuttgart, Germany
[2]Institute of Materials Research, German Aerospace Center
Cologne, Linder Höhe, D-51147 Köln, Germany

received October 18, 2013; received in revised form December 9, 2013; accepted December 18, 2013

**Abstract**

**Thanks to its low cost and high flexibility, in the last few years the winding technique has been successfully adapted for the production of complex Ceramic Matrix Composite (CMC) components with load-oriented fibre alignment. Since the winding angle can be adjusted in any direction (from 0° to 90°) during the fabrication process, it is important for the design of components to evaluate the elastic properties of CMCs as a function of the winding angle.**

**In this study, an inverse method based on the Classic Laminate Theory (CLT) has been used for the prediction of the elastic properties, i.e. Young's modulus, shear modulus and Poisson's ratio, for a wound oxide CMC material, called WHIPOX® (Wound HIghly Porous OXide ceramic matrix composite). For this purpose the characteristics of an equivalent unidirectional layer (UD-layer) with consideration of fibre volume content (FVC) and porosity were calculated. On the basis of microstructural analysis the computed WHIPOX® UD properties have been divided into two sets of elastic properties for small (below 30°) and large winding angles (30° and above). Full coverage of the mechanical properties in different wound orientations, non-orthogonal with ±3°/±87°, ±15°/±75°, ±30°/±60° and orthogonal with ±45° and 0°/90°, were evaluated with in-plane tension, and Iosipescu-shear tests. A good correlation between experimental and analytically calculated results is shown in this paper.**

*Keywords: Ceramic matrix composite, fibre orientation, elastic properties, inverse laminate theory, equivalent unidirectional layer*

## I. Introduction and Objective

The winding technique for the production of fibre-reinforced Ceramic Matrix Composites (CMC) components has been widely applied in recent years, especially for the production of components with rotational symmetry such as tubes, nozzles or combustion chambers for process technology or aerospace applications [1–3]. Because of the high flexibility of this method, the winding angle can be adjusted in any desired direction (from 0° to 90°) for load-optimized fibre orientation. The variability of the fibre arrangement requires advanced models for the evaluation and prediction of the elastic properties of CMC components. Based on Classical Laminate Theory (CLT) or on a Representative Volume Unit (RVU), various methods for the evaluation of the mechanical behaviour of wound and braided materials, especially for composites with polymeric matrix, have been discussed in a number of studies. These numerical and analytical attempts showed good applicability for forecasting the elastic properties[4–8].

Owing to the lack of matrix, fibre and interface properties within the composite material, the modelling of the mechanical behaviour of wound CMCs, such as WHIPOX®, is particularly difficult. Especially the matrix properties, considering the specific matrixporosity and micro-crack density, are different from pure matrix properties. Furthermore, the production and characterization of unidirectional layers (UD-layers) for CMCs is also critical because non-typical unhindered shrinkage of the matrix transverse to the fibres during processing leads to material that cannot be considered as being representative material for CLT.

Alternatively, experimental and theoretical investigations for the determination of the properties of wound CMCs by an inverse approach based on CLT are discussed in [9, 10].

The present study pursues the objective of predicting the elastic properties of wound composites with varying winding angles with an inverse approach. An equivalent UD-layer was calculated with an analytical approach with consideration of fibre volume content (FVC), porosity and microstructures at different winding angles. The model has been demonstrated based on experimental investigation of a wound oxide CMC material, WHIPOX® (Wound HIghly Porous OXide ceramic matrix composite).

## II. Modelling Approach

A key advantage of the wound CMCs is gained by its in-plane anisotropic material behaviour, which is strong-

* Corresponding author: yuan.shi@dlr.de

ly dependent on the winding angle $\theta$, defined between the longitudinal axis *X* of the wound preforms and the direction of the fibre tows (Fig. 1a). In order to realize the prediction of mechanical properties of wound CMCs, which can be built up using identical repetitive elements, two different concepts, either by application of a unit cell-model or an equivalent UD-layer can be achieved. Both concepts are based on the homogenization of material properties. By using experimentally determined parameters from the laminate it is more efficient to use a model with equivalent UD-layer approach. For this purpose, a single non-orthogonal wound CMC-Double-Layer with crossing points, such as WHIPOX® with wound angle $\pm\theta°$ in Fig. 1a is replaced by two superimposed UD-layers with angle $+\theta$ and $-\theta$ in Fig. 1b. These UD-layers with the half thickness of a symmetric double layer have identical mechanical and geometrical properties in the local coordinate system in fibre orientation and perpendicular to it. Owing to the fact that the fibre and matrix properties are unknown, the elastic properties of the equivalent UD-layer are calculated by using the inverse operation of CLT and Cartesian transformation. Through the stacking of those equivalent UD-layers with the orientation $\pm\theta$, an equivalent layered composite (Fig. 1c) is designed which has orthotropic properties. Finally, the equivalent UD-layers allow the modelling of any other fibre orientation and stacking sequence.

With the assumption that material properties of a symmetric laminated composite are homogeneous on a macroscopic scale and that the material exhibits a linear elastic behaviour, the stiffness matrix $[\bar{Q}]$ of a multilayer laminate can describe the relationship between strains $\{\varepsilon°\}$, curvature $\{\kappa\}$, occurring stress $\{N\}$ and moments $\{Mo\}$ in the laminate under in-plane loading [11]:

$$\begin{Bmatrix} \{N\} \\ \{Mo\} \end{Bmatrix} = \begin{bmatrix} [S] & [C] \\ [C] & [B] \end{bmatrix} \begin{Bmatrix} \{\varepsilon°\} \\ \{\kappa\} \end{Bmatrix} \quad (1)$$

The individual sub-matrices of $[\bar{Q}]$ are: strain stiffness [S], coupling stiffness [C] and bending stiffness [B]. They are determined from the stiffness matrix of a single layer:

$$([S],[C],[B]) = \sum_{k=1}^{n} \int_{h_{k-1}}^{h_k} (1, z_k, z_k^2) \left[\bar{Q}\right]_k dz \quad (2)$$

Where $n$ is the number of layers, $h_k$ and $h_{k-1}$ represent the start- and end-coordinates of each individual layer $k$. The reduced stiffness matrix $[\bar{Q}]$ along the global coordinate system (*X*- and *Y*-axis in Fig. 1a) will be transformed in the material stiffness matrix $[\bar{Q}]$ as follows [11]:

$$[Q] = [Ma]^{-1} [\bar{Q}] \quad (3)$$

$[Ma]^{-1}$ is inverse of matrix [Ma], which establishes the relationship between the global coordinate system and material coordinate system (*1*- and *2*-axis) with rotation angle $\theta$ (angle from axis x to 1 in Fig. 1a):

$$[Ma] = \begin{bmatrix} m^4 & n^4 & 2m^2n2 & 4m^2n^2 \\ n^4 & m^4 & 2m^2n^2 & 4m^2n^2 \\ m^2n^2 & m^2n^2 & m^4n^4 & -4m^2n^2 \\ m^2n^2 & m^2n^2 & -2m^2n^2 & (m^2n^2)^2 \end{bmatrix} \quad (4)$$

where $m = cos\theta$ and $n = sin\theta$.

The material stiffness matrix [Q] of an equivalent UD-layer with *1*-axis in fibre direction and *2*-axis in transverse direction (Fig. 1b) can be calculated for the plane stress state as follows:

$$[Q] = \begin{bmatrix} Q_{11} & Q_{12} & 0 \\ Q_{12} & Q_{22} & 0 \\ 0 & 0 & Q_{66} \end{bmatrix} \quad (5)$$

The elastic constants of the UD-layer can be determined with the following equations:

$$E_1 = Q_{11} - \frac{Q_{12}^2}{Q_{22}} \qquad E_2 = Q_{22} - \frac{Q_{12}^2}{Q_{11}}$$

$$\upsilon_{12} = \frac{Q_{12}}{Q_{22}} \qquad G_{12} = Q_{66}$$

The Young's modulus of the single layer in fibre direction is denoted by $E_1$ and perpendicular thereto by $E_2$. $\upsilon_{12}$ is the Poisson's ratio and $G_{12}$ is the shear modulus.

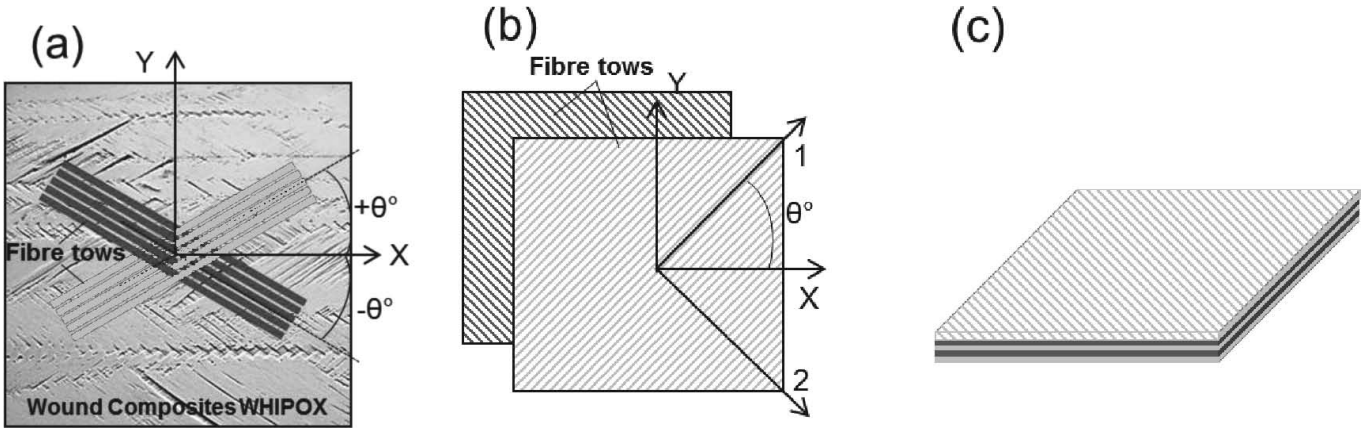


**Fig. 1:** Modelling approach for wound fibre composites ceramics: (a) CMC material WHIPOX® with schematic representation of winding structure, winding angle $\pm\theta°$; (b) Equivalent UD-layers with local coordinate system, 1-axis in fibre direction and 2-axis in perpendicular direction; c) Equivalent composite structure with UD-layers.

## III. Experimental

### *(1) Material description*

For the experimental tests the wound oxide/oxide composite WHIPOX® was selected. Plates with different wound angles (±3°/±87°, ±15°/±75°, ±30°/±60° and ±45°, 0°/90°) were produced at the Institute of Materials Research of the German Aerospace Center in Cologne. The manufacturing process for even plates is carried out in five steps: matrix infiltration of fibre tows, winding with defined angle to a cylindrical preform, cutting and flat lay-up, drying and then sintering for about 1 h at temperatures < 1300 °C [1]. Fig. 1a shows the surface of a WHIPOX® plate with a winding angle of ± 30°. The average values from tested composites – the fibre volume content, the density and the open porosity measured with the Archimedes method – are summarized in Table 1.

**Table 1 :** Material parameters for all investigated plates.

| Fibre | Matrix | Average fibre volume content [%] | Average density [g/cm³] | Average porosity [%] |
|---|---|---|---|---|
| N610 ($Al_2O_3$) | $Al_2O_3$ | 39.3 | 2,87 | 27.1 |

### *(2) Experimental procedure*

The material properties were evaluated in an in-plane tensile and Iosipescu shear test [12]. The test samples were cut from flat panels with fibre orientations of ±3°/±87°, ±15°/±75°, ±30°/±60°, ±45° and 0°/90° relative to the specimen longitudinal axis. Specimen geometries and dimensions are shown in Fig. 2. Tensile specimens were produced with reduced cross-section in the gauge area in order to prevent failure in the clamping section and assure failure in the centre region. All the experiments were performed at room temperature in air under quasi-static loading. For the tensile test the longitudinal and the transverse strains were measured with strain gauges. In the shear tests the strain was evaluated from strain gauges in the +45° and in the -45° directions relative to the shear loading direction. All the tests were performed up to failure on an universal testing machine (Zwick) at a controlled cross-head speed of 1 mm/min. The failure stress was calculated from the maximum load. For statistical confirmation three to five tensile and shear samples per series were tested.

## IV. Results and Discussion

### *(1) Experimental results*

Typical tensile stress-strain curves of the investigated configurations are shown in Fig. 3, which presents the longitudinal and transverse strains. The indications +30°/-30° and +60°/-60° and +45°/-45° and 0°/90° denote the angles between the fibre and loading direction. The stress-strain response of WHIPOX® strongly depends on the loading direction. Under ±30° and 0°/90° orientation the composites show an almost linear behaviour with higher stiffness and strength. Since the fibres are orientated close to the loading direction, the matrix is able to transfer the applied load to the fibres. In contrast, under ±60° and ±45° loading the composite stiffness is low and non-linear behaviour already occurs at low stresses, which indicates that damage of matrix and interface is leading to a significant degradation of the composite properties in this loading direction.

The determination of the elastic constants was conducted using a linear fit of the initial linear region of the stress-strain curves. The measured elastic constants of WHIPOX® with non-orthogonal and orthogonal wound angle are summarized in Table 2. The indices *X* and *Y* correspond to the indications from Fig. 1a. For orthogonally wound WHIPOX®, the Young's modulus $E_x$ is equal to $E_y$.

### *(2) Analytical results and microstructural analysis*

In order to predict the elastic constants of wound WHIPOX®, the modelling approach from Section 2 was applied. The elastic parameters of an equivalent UD-layer ($E_1$, $E_2$, $\nu_{12}$, $G_{12}$) were calculated based on the experimental data (Table 2) for different non-orthogonal fibre orientations. In order to consider the effect of manufacturing fluctuations at each winding angle, each computed $E_1$ was scaled by the average fibre volume content (approx. 39.3 % in Table 1) of all tested specimens as fibre properties dominate the properties in 1-direction. On the other hand, $E_2$ was scaled by the average porosity (approx. 27.1 % in Table 1) as the porosity has the main impact on $E_2$. The calculated properties of the equivalent UD-layers were used for the calculation of elastic properties of orthogonal orientations ±45° and 0°/90°.

**Table 2 :** Elastic constants in directions X and Y obtained from tensile and shear tests for WHIPOX® with different winding angle.

| Average elastic constants with standard deviation | | | | | |
|---|---|---|---|---|---|
| | Orientation | $E_x$ [GPa] | $E_y$ [GPa] | $\nu_{xy}$ [-] | $G_{xy}$ [GPa] |
| Non-orthogonal | ±3°(±87°) | 214.0 ± 10.0 | 117.0 ± 7.0 | 0.19 ± 0.01 | 41.9 ± 0.9 |
| | ±15°(±75°) | 202.0 ± 7.3 | 114.2 ± 3.3 | 0.25 ± 0.03 | 51.4 ± 6.9 |
| | ±30°(±60°) | 134.4 ± 9.2 | 65.4 ± 9.7 | 0.39 ± 0.05 | 50.7 ± 11.4 |
| Orthogonal | ±45° | 100.5 ± 1.13 | 100.5 ± 1.13 | 0.35 ± 0.11 | 59.2 ± 2.1 |
| | 0°/90° | 122.9 ± 1.2 | 122.9 ± 1.2 | 0.12 ±0.01 | 43.6 ± 8.0 |

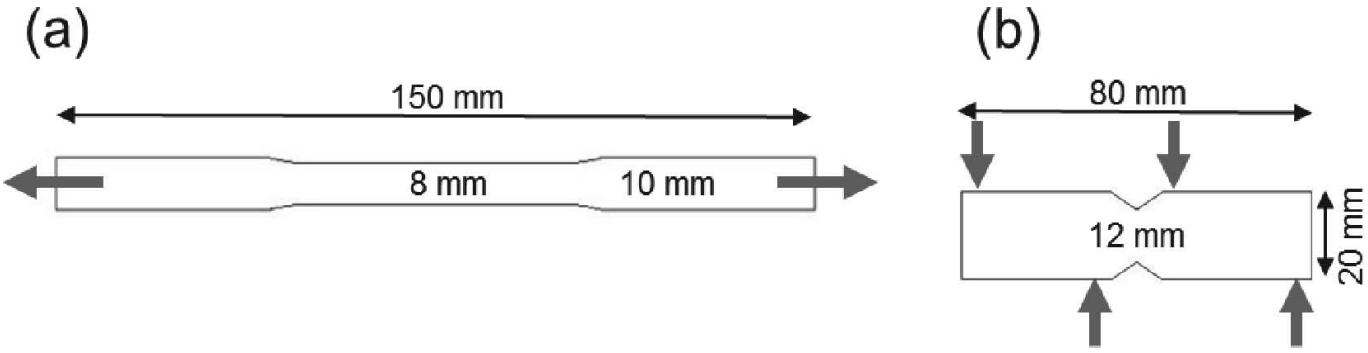


**Fig. 2:** Specimen geometry and dimensions used for the experiments: a) Tensile specimen with dimensions of 150×10(8)×5 mm³; b) Iosipescu specimen with dimensions of 80×20(12)×5 mm³ and notch angle of 110°.

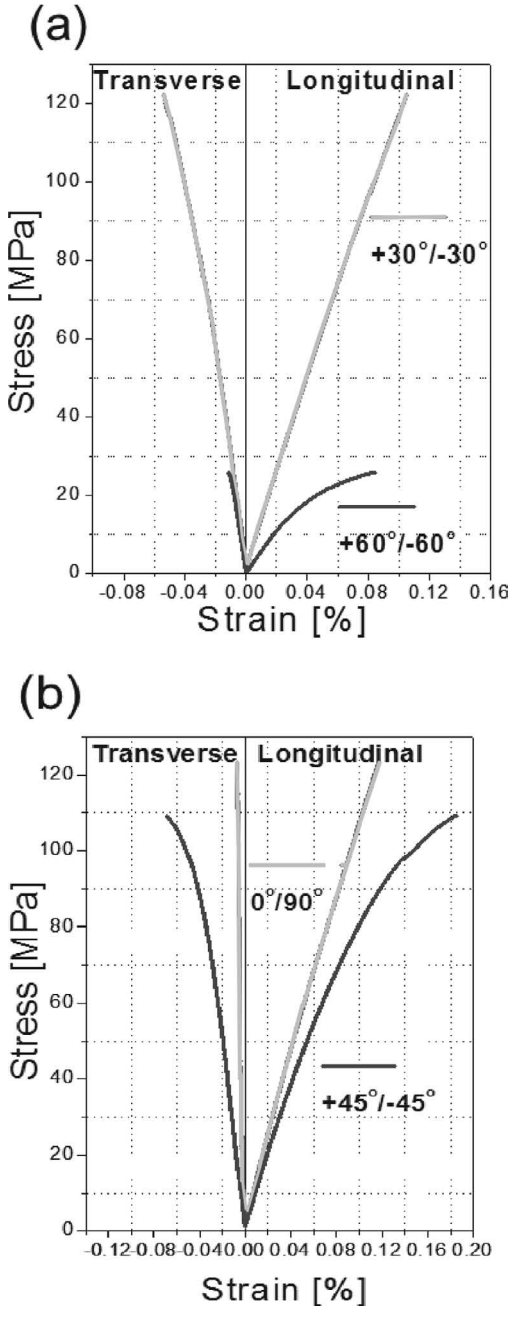


**Fig. 3:** Typical tensile stress-strain curves from longitudinal and transverse strain gauge measurement for a) fibre orientations ±30° and ±60°; b) fibre orientation ±30°and 0°/90°.

From the experimental results of non-orthogonal orientations in Table 2, four independent elastic constants of equivalent UD-layers were evaluated: $E_1$, $E_2$, $\upsilon_{12}$, $G_{12}$.

In contrast to the other three constants of the equivalent UD-layer, the Young's modulus transverse to the fibre direction strongly depends on the winding angle of tested composites: the average value $E_2$ of large angles such as ±30° and above is about only half of the ±3°or ±15°. This behaviour can be explained by the shrinkage of matrix cracks. During the sintering process, shrinkage of the matrix will be blocked by the stiff fibres. The maximum hindering of shrinkage is reached at high winding angles, e.g. ±45° winding. This leads to cracking of the matrix during sintering and thus to reduced Young's moduli in the transverse direction $E_2$. μ-Computer-Tomography (CT) was applied for the analysis of shrinkage cracks. Some cracks are clearly visible for the sample with orientation ±45° in Fig. 4a. The crack density will be calculated for different winding angles. In case of ±45° the density of cracks equals approx. 8.7 per mm². In contrast, no shrinkage cracks are visible for orientation of ±15° (Fig. 4b).

Based on the microstructure analysis, no monotonic increase of the crack density in relation to winding angle can be observed: WHIPOX® with a winding angle of ±45° and ±30° (crack density equals approx. 6.7 per mm²) shows similar crack distribution (Fig. 4a and c). No cracks were observed for smaller winding angles. Therefore the evaluation of the properties of WHIPOX® was divided into two classes: WHIPOX® with matrix cracks and WHIPOX® without matrix cracks.

## V. Discussion

Since the inverse laminate theory showed that the shrinkage cracks have a distinct impact on Young's modulus $E_2$, but not on the other elastic constants, two UD-material parameter sets with different $E_2$ values were defined. The UD-layer parameter set UD-WC (UD-layer with cracks) was defined for the angles ±45° and ±30° and a second parameter set, UD-NC (UD-layer no cracks), with higher $E_2$ for the angles ±15° and smaller (Table 3). $E_1$, $\upsilon_{12}$ and $_{12}$ are averaged values from all fibre orientations for UD-WC and UD-NC. $E_2$ was calculated from the respective associated winding angles. The $E_2$ value (56.2 GPa) for UD-WC is reduced to around 50 % of $E_2$ from UD-NC (107.8 GPa) owing to shrinkage micro-cracks.

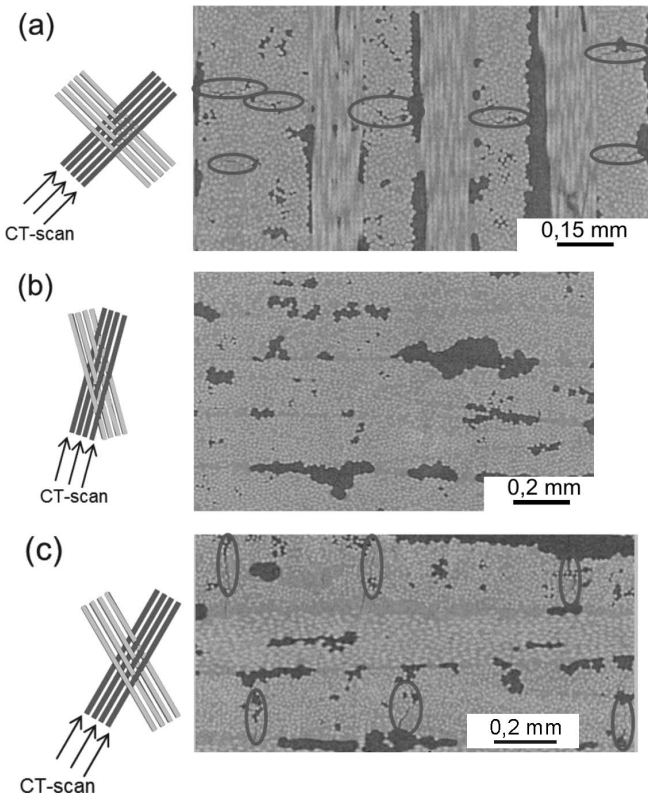


**Fig. 4 :** CT-images of the WHIPOX® material with different fibre orientations: a) Winding angle ±45°, the areas marked in red show the shrinkage cracks, which are perpendicular to the fibre orientation; b) Winding angle ±15°, there are no shrinkage cracks visible; c) Winding angle ±30°, similar crack density and distribution as ±45°.

**Table 3 :** Calculated elastic constants for equivalent UD-layers with consideration of fibre volume content and porosity; UD-WC corresponds to winding angles of ±45° and ±30° and UD-NC applies to angles ±15° and smaller.

| | $E_1$ [GPa] | $E_2$ [GPa] | $\nu_{12}$ [-] | $G_{12}$ [GPa] |
|---|---|---|---|---|
| UD-WC | 211.2 | 56.2 | 0,20 | 40.0 |
| UD-NC | 211.2 | 107.8 | 0,20 | 40.0 |

The elastic properties of the orthogonal (±45° and 0°/90°) wound WHIPOX® material were determined on the basis of the calculated elastic constants for the equivalent UD-layer (Table 3) with CLT. The results for UD-WC and UD-NC are compared with the experimental values and listed in Table 4. The same results are visualized in Fig. 5. Following the analysis of shrinkage cracks in Fig. 4, the data set of UD-WC is applicable for the computation of orthogonal winding angles ±45° and 0°/90°. A very good correspondence is obtained for the measured and predicted Young's moduli $E_x$, $E_y$ and shear modulus $G_{xy}$ with maximum of 8 % difference when the parameters of UD-WC are applied. In general, higher elastic constants $E_x$, $E_y$ and $G_{xy}$ are calculated using UD-NC with winding angles ±45° and 0°/90°. The predicted $G_{xy}$ using UD-WC and UD-NC for orthogonal wound WHIPOX® 0°/90° are the same because of the identical $G_{12}$ of both UD classes and reached a good agreement with the experimental result. However, slight differences for the Poisson's ratio are predicted with the use of UD-WC. This may be explained by the difficulty of the experimental evaluation of Poisson's ratio, especially for 0°/90° composites. It's probably not precise enough owing to the marginal transverse strains (Fig. 3b).

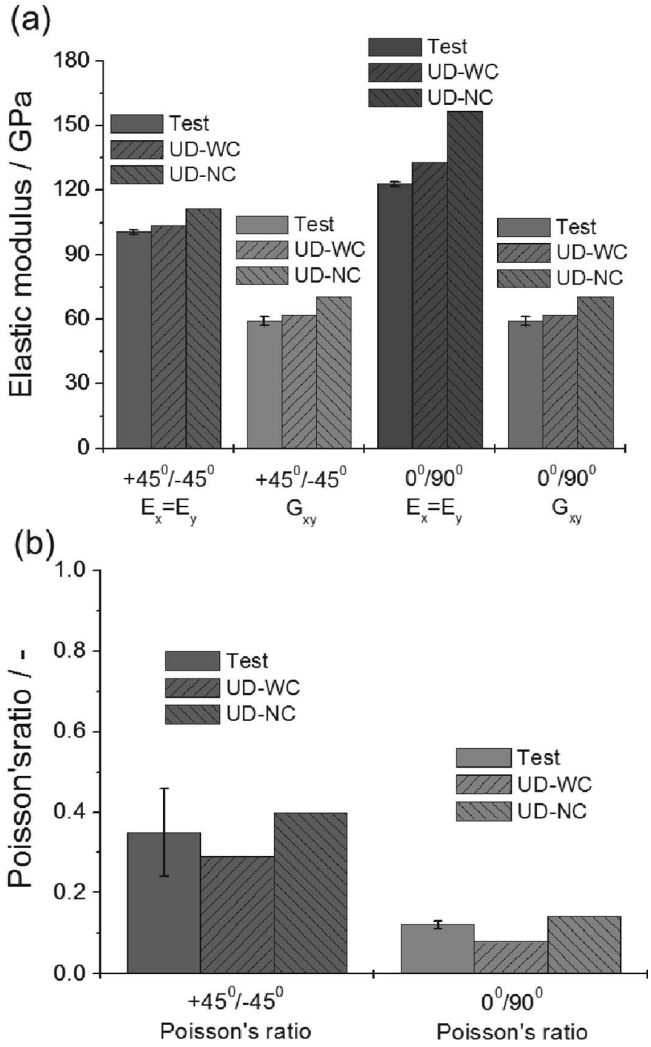


**Fig. 5 :** Comparison of calculated elastic constants using UD-WC and UD-NC with test results for orthogonally wound WHIPOX® ±45° and 0°/90°: a) Young's moduli and shear modulus; b) Poisson's ratio.

Based on the good agreement between experiments and modelling results, calculations were performed for symmetric wound WHIPOX® composites (±θ° in Fig. 1c) with the elastic constants for the equivalent UD-layers of UD-WC and UD-NC in Table 3. The elastic constants computed from the different parameter sets UD-WC and UD-NC are plotted in Fig. 6 in dependence of the winding angle. The different $E_2$ values of UD-WC and UD-NC have a distinct effect on $E_x$, $E_y$, which results in good agreement with the respective experimental data. In Fig. 6a experimental data of ±45° and ±30° and predicted elastic constants using UD-WC show a difference of only around 10 %. More than 50 % of difference is predicted by using the same UD parameters for lower winding angles. In contrast, using suitable UD-NC parameters for the prediction of composites with ±3° and ±15° fibre angles results in differences less than 9 % (Fig. 6b).

**Table 4 :** Comparison of calculated elastic constants using UD-WC and UD-NC with experimental results for orthogonally wound WHIPOX® ±45° and 0°/90°.

| Fibre orientation | | $E_x = E_y$ [GPa] | $\nu_{xy}$ [-] | $G_{xy}$ [GPa] |
|---|---|---|---|---|
| ±45° | Experimental results | 100.5 ± 1.1 | 0.35 ± 0.11 | 59.2 ± 2.1 |
| | Calculated using UD-WC | 103.5 | 0.29 | 61.9 |
| | Calculated using UD-NC | 111.6 | 0.40 | 70.4 |
| | | | | |
| 0°/90° | Experimental results | 122.9 ± 1.2 | 0.12 ± 0.01 | 43.6 ± 8.0 |
| | Calculated using UD-WC | 133.2 | 0.08 | 40.0 |
| | Calculated using UD-NC | 156.8 | 0.14 | 40.0 |

The comparison of computed elastic constants and experimentally measured properties of the WHIPOX® material shows that the separation into shrinkage-cracked and crack-free matrix in combination with ILT is useful for the design of these composites.

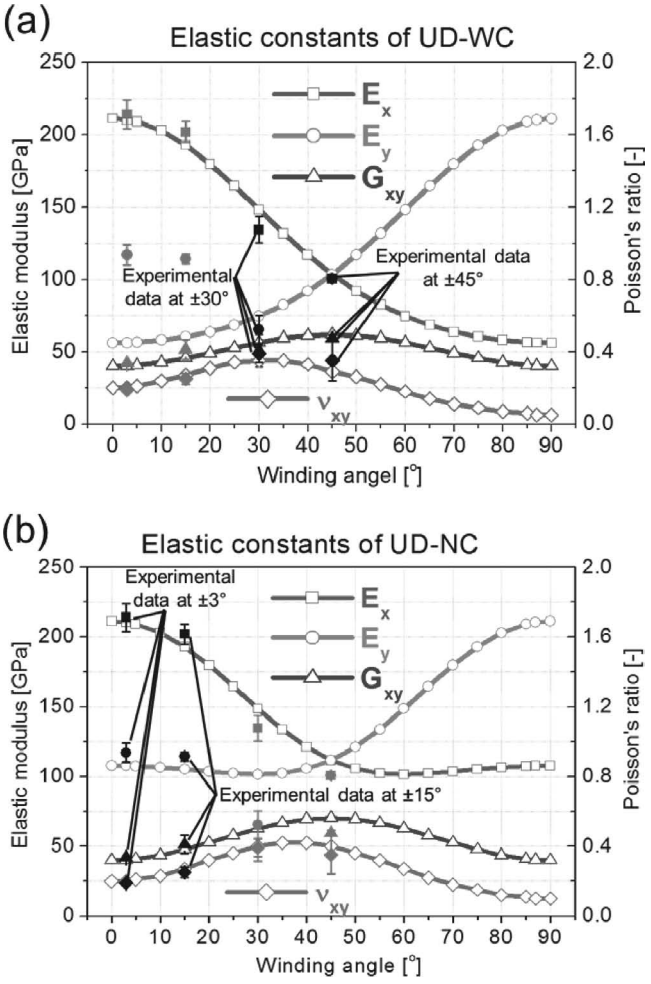


**Fig. 6 :** Experimental data and predicted variation of the elastic constants for wound WHIPOX® material depending on the winding angle: a) Calculated with UD-WC and b) Calculated with UD-NC.

## VI. Conclusions

In this paper, an approach for the evaluation and determination of the elastic properties of an equivalent virtual UD-layer was presented. On the basis of experimental data and computer-tomography-based analysis of microstructures for different winding angles, virtual WHIPOX® UD properties have been calculated and divided into two groups: UD properties with shrinkage cracks for large reinforcing angles and UD properties without cracks for small reinforcing angles. Based on the good agreement between experiments, analysis of shrinkage cracks and modelling results, it could be shown that the analytical approach allows very accurate prediction of the in-plane elastic properties for CMC laminates and will help to develop CMC structures that are more adequate to meet stiffness requirements.

## References

1 Göring, J., Hackemann, S., Kanka, B.: WHIPOX®: A fibre-reinforced oxide ceramic material for high-temperature long-term applications, (in German), *Mat.-wiss. u. Werkstofftech.*, **38**, [9], 766 – 772, (2007).

2 Schmidt, S., Beyer, B., Knabe, H., Immich, H., Meistring, R., Gessler, A.: Advanced ceramic matrix composite materials for current and future propulsion technology applications, *Acta Astronaut.*, **55**, [3 – 9], 409 – 420, (2004).

3 Herbell, T.P., Eckel, A.J.: Ceramic matrix composites for rocket engine turbine applications, *J. Eng. Gas. Turb. Power,* **115**, [1], 64 – 69, (1993).

4 Huang, Z.M.: The mechanical properties of composites reinforced with woven and braided fabrics, *Compos. Sci. Technol.*, **60**, [7], 479 – 498, (2000).

5 Carey, J., Munro, M., Fahim, A.: Longitudinal elastic modulus prediction of a 2-D braided fiber composite, *J. Reinf. Plast. Comp.*, **22**, [9], 813 – 831, (2003).

6 Potluri, P., Manan, A.: Mechanics of non-orthogonally interlaced textile composites, *Compos. Part A.*, **38**, [4], 1216 – 1226, (2007).

[7] Srikanth, L., Rao, R.M.V.G.K.: Concurrent studies on braided and filament wound carbon fiber composites – a comparative appraisal, *J. Reinf. Plast. Comp.*, **30**, [16], 1359 – 1365, (2011).

[8] Xu, L., Kim, S.J., Ong, C.H., Ha, S.K.: Prediction of material properties of biaxial and triaxial braided textile composites, *J. Compos. Mater.*, **16**, [18], 2255 – 2270, (2012).

[9] Zebdi, O., Boukhili, R., Trochu, F.: An inverse approach based on laminate theory to calculate the mechanical properties of braided composites, *J. Reinf. Plast. Comp.*, **28**, [23], 2911 – 2930, (2009).

[10] Tushtev, K., Koch, D., Grathwohl, G.: Elastic properties of braided ceramic matrix composites, *Int. J. Mater. Res.*, **99**, [11], 1262 – 1267 (2008).

[11] Chawla, K.K.: Ceramic matrix composites, Chapman & Hall, London. 1993.

[12] Iosipescu, N.: New accurate procedure for single shear testing of metals, *J. Mater.*, **2**, 537 – 566, (1967).